Kinetics and Catalysis, Vol. 45, No. 3, 2004, pp. 429–435. From Kinetika i Kataliz, Vol. 45, No. 3, 2004, pp. 455–462.

CATALYTIC REACTION MECHANISMS

Combustion of Carbon Black Catalyzed by Transition Metal-Promoted Y_2O_3–CeO_2–ZrO_2 Solid Solutions[1]

J. F. Lamonier*, S. P. Kulyova, E. A. Zhilinskaya*, B. G. Kostyuk**, V. V. Lunin**, and A. Aboukaïs***

** Laboratoire de Catalyse et Environnement, Université du Littoral-Côte d'Opale, 59140 Dunkerque Cedex, France*

*** Laboratory of Catalysis and Gas Electrochemistry, Department of Chemistry, Moscow State University, Vorob'evy gory, Moscow, 119899 Russia*

Received December 23, 2002

Abstract—The activity of M-free and M-loaded $10YO_{1.5}$–$10CeO_2$–$80ZrO_2$ solid solution (M = Cu, V, or W) towards carbon black combustion was studied using TG/DTA and TPO techniques. It was demonstrated that all studied catalysts lower the temperature of carbon black combustion. The selectivity of the catalytic reaction in CO_2 formation was 100%. It was evidenced that the fast oxidation of carbon at lower temperatures, observed only in the TG/DTA apparatus, was due to heat- and mass-transfer limitations, resulting in a runaway reaction. Using TPR technique, it was shown that, in the temperature range of DTA curve, oxygen on the catalyst surface was rather reactive (and, therefore, it could be easily released by support for the oxidation of carbon), whereas the reactivity of bulk oxygen was negligible. The activity of the metal-loaded $10YO_{1.5}$–$10CeO_2$–$80ZrO_2$ (Y-10) samples varied according to the following sequence: Cu/Y-10 > V/Y-10 > W/Y-10. For Cu- and V-containing catalysts, a contribution of a surface redox mechanism in reaction was proposed by comparing EPR spectra of pure catalysts with those of the samples (catalysts mixed with carbon black) after catalysis.

1. INTRODUCTION

Internal-combustion engines (both gasoline- and diesel-fueled) are known to significantly contribute to air pollution, which has a damaging impact on the environment and is suspected to cause global climate changes. Ecological benefits of diesel engines, such as low greenhouse gas emissions, are balanced by high emission of NO_x and solid particles, mainly soot.

Soot emission can be controlled by placing a porous ceramic filter downstream for the collection of solid particles. Soot, deposited on the filter, must be periodically burnt down to avoid an increase of backpressure in exhaust gas. However, such a regeneration of the filter requires high temperatures (higher than those of the exhaust gases and, hence, the filter). There are two principal approaches to the solution of the regeneration problem. The first way is to increase the filter temperature using special burners and electric heaters [1]; the second is to lower the soot ignition temperature using oxidation catalysts such as single metal oxides and mixed oxide systems [2–4] or eutectic mixtures based on oxides [5, 6].

It is obvious that the catalytic regeneration of the filter is more suitable than the thermal one since it does not require additional car equipment. Oxidation catalysts can be either added to the fuel in the form of soluble compounds or coated onto the internal surface of the filter [1, 7]. In the former case, the catalyst is incorporated into the soot particles during their formation ensuring good contact between active components and soot particles and this results in a high degree of soot conversion both into the waste gas flow directed to the filter and in the filter itself. In the latter case, the accumulated soot is oxidized in the filter.

In recent years, special attention has been focused on the application of ceria (CeO_2), structurally doped with zirconia (ZrO_2), for the treatment of emissions from car engines, including diesel exhaust. In comparison with pure CeO_2, the thermal stability, redox properties, and catalytic activity of these solids are strongly enhanced. These special properties are explained by the substitution of Ce^{4+} by Zr^{4+} into the CeO_2 lattice, which favors the creation of structural defects and results in the acceleration of oxygen diffusion. The higher mobility and, hence, reactivity of lattice oxygen is related to the phase modification of CeO_2–ZrO_2 oxides from tetragonal into cubic form. Moreover, the incorporation of yttrium (as Y^{3+}) in the CeO_2–ZrO_2 lattice promotes the stabilization of a single homogeneous cubic phase (especially in $10YO_{1.5}$–$10CeO_2$–$80ZrO_2$ [8]). The presence of anionic vacancies on the Y_2O_3–CeO_2–ZrO_2 ternary oxide surface provides special interaction with the impregnated active phase, which could induce particular catalytic activity [9].

The purpose of this work is to study the combustion of carbon black in the presence of $10YO_{1.5}$–$10CeO_2$–$80ZrO_2$ ternary oxide doped with transition metals (Cu, V, or W), to elucidate the role of the oxide support (which exists in a pure cubic phase and, therefore, it is expected to be an efficient oxygen exchanger) in the

[1] This article was submitted by the authors in English.

reaction, and to determine the centers of the catalysts responsible for their activity.

2. EXPERIMENTAL

2.1. Preparation of Samples

The support of the following composition (in mol %) $10YO_{1.5}$–$10CeO_2$–$80ZrO_2$ (denoted as Y-10) was prepared by coprecipitation. It was synthesized by means of adding NH_4OH solution to a solution containing a mixture of $Y(NO_3)_3$, $Ce(NO_3)_3$, and $ZrO(NO_3)_2$ salts with the desired Y : Ce : Zr ratio and a total concentration of 0.2 mol/l ions (the pH was about 10.5–11). The prepared gel was washed with deionized water and then with an ethanol solution (40%), dried at 373–393 K (5 h), and calcined at 823 K in a muffle furnace (5 h).

The catalysts with 0.5, 1, or 3 wt % of metal were prepared by the impregnation of the support with a solution of $Cu(NO_3)_2 \cdot 6H_2O$, NH_4VO_3, or $(NH_4)_{10}H_2(W_2O_7)_6 \cdot 4H_2O$ followed by drying and calcination in air at 523, 723, and 973 K for Cu-, V-, and W-containing samples, respectively.

2.2. Catalytic Tests

The combustion of carbon black (CB), N330 supplied by Degussa, model of soot [7] (BET surface area is 80 m^2/g; content of hydrocarbons, C_{12}–C_{22} alkanes, is 1 wt %), was studied simultaneously with thermogravimetric (TGA) and differential thermal analyses (DTA) using a Netzsch STA 409 apparatus. Some of the samples were also investigated with the temperature-programmed oxidation (TPO) technique. For both experiments, we used 0.05 g of the mixtures of catalyst with CB (80 and 20 wt %, respectively), which were obtained by mechanical mixing in a ball miller for 40 min. Before mixing, all the catalysts were activated at 823 K.

In TG/DTA experiments, the reaction mixture was loaded in an alumina crucible (cylindrical shape and 4 mm height) and heated from ambient temperature to 873 K (5 K/min) in air flow (75 ml/min). The analysis of combustion products was performed using a Varian 3600 chromatograph coupled with a thermobalance [4]. Two chromatography columns (one inside of other: CTRI Alltech) were used to separate the components of the gas mixture (air, O_2, N_2, CO, and CO_2). The outer column was filled with molecular sieve 5A, whereas the inner one was filled with adsorbent Porapak Q. The operating conditions were as follows: columns temperature was 348 K, thermoconductivity detector temperature was 423 K (~180 mA), carrier-gas was helium (20 ml/min).

TPO tests were carried out in a flow device equipped with a quartz fixed bed reactor placed into a tube furnace, an air pump, and a loop with zeolite 4A for the removal of water. Air flow (75 ml/min) passed through the samples while the furnace temperature was raised from room temperature to 873 K (5 K/min). CO_2 was registered with the use of acoustic gas analyzer "Megakon" situated at the exit of the gas flow from the reactor. In these experiments, CO was not analyzed since it was not found in the products of CB combustion during preliminary DTA tests.

2.3. Temperature Programmed Reduction (TPR)

TPR of the catalysts was carried out in a flow device equipped with a system of gas preparation and purification, a quartz reactor situated into a tube furnace, and a thermal conductivity detector. In order to minimize the contribution of surface impurities and water, before the experiments, the samples (0.1 g) were calcined in O_2 flow at 723 K (1 h). After cooling to room temperature (in an Ar flow), the samples were reduced with H_2 (5 vol % in Ar). The flow rate was 23 ml/min, and the heating rate was about 13 K/min.

2.4. Electron Paramagnetic Resonance (EPR)

EPR spectra were recorded at 293 and 77 K with a Bruker EMX spectrometer operating in the *X* band microwave frequency (~9.5–9.7 GHz). The magnetic field was modulated at 100 kHz. The *g*-factor values were determined by simultaneously measuring the microwave frequency and the magnetic field. All EPR spectra were treated with the Bruker WINEPR program, and the Bruker SimFonia program was used to simulate the EPR spectra.

3. RESULTS AND DISCUSSION

3.1. Catalytic Oxidation of Carbon Black

The activity of the catalysts was considered from the standpoint of their ability to decrease the combustion temperature of CB in air, which in the absence of catalysts occurs in the ~800–900 K range [4]. The temperature of the first DTA peak was chosen as a characteristic of the catalytic activity of the samples. The data of thermal experiments are listed in Table 1. Note that, in all cases, selectivity of the reaction in CO_2 formation was 100%.

All the DTA curves consisted of two exothermic peaks. The first peak was narrow and sharp whereas the second one, appearing at higher temperatures, was broad and smooth (for example, DTA curve for 3% Cu/Y-10 in Fig. 1, curve *1*). The most important weight loss on the TGA curves was observed in the temperature range corresponding to the first DTA peak (a fast process), whereas a smaller weight loss was found for the temperature area of the second DTA peak (a slow process). Pruvost *et al.* [4] have already explained these two oxidation phenomena: the first DTA peak is related to the combustion of CB particulates, which are in tight contact with the catalyst, whereas the second peak is instead assigned to the combustion of weakly bonded carbon particulates.

Table 1. Values of temperature of the first DTA maximum (T_{max}) and weight loss obtained from DTA–TGA experiments in air flow for CB + catalyst mixtures

Sample	Surface area, m^2/g	T_{max}, K	Weight loss for first and second DTA peaks, %		
			first peak	second peak	both peaks
CB + Y-10	70	749	12.2	7.2	19.4
CB + 0.5%Cu/Y-10	55	712	15.5	7.4	22.9
CB + 1%Cu/Y-10	43	703	15.6	6.4	22.0
CB + 3%Cu/Y-10	38	694	16.0	4.7	20.7
CB + 3%V/Y-10	40	734	12.1	8.3	20.4
CB + 3%W/Y-10	54	740	10.4	9.1	19.5

Figure 1 compares the DTA curve (curve *1*) with the DTGA curve (time derivative of the TGA curve) (curve *2*) for a 3% Cu/Y-10 sample. A very good mutual accordance between both curves indicates that each of the two DTA peaks is a result of a chemical reaction, which is not accompanied by other chemical reactions or physical transformations. Indeed, in the case of several chemical reactions in the absence or presence of physical transformations, the corresponding DTA peak is the result of thermal effects of all these processes, and, therefore, the DTA and DTGA curves must show different changes. In our experiments, these curves always showed identical changes. It is obvious that the presence of both DTA peaks is related to the oxidation of CB. The evidence is the formation of the combustion product (CO_2) in the temperature ranges of both the first and second DTA peaks as well as the appearance of the curve corresponding to the rate of CO_2 formation (Fig. 1, curve *3*), coinciding according to its shape and temperature position with the appropriate DTA curve (Fig. 1, curve *1*).

However, it has been found that the first/second peak area ratio for DTA curves is not the same as for curves of temperature dependence of the rate of CO_2 formation (see, e.g., Fig. 1, curves *1* and *3*). In fact, a correlation between the areas of the first and second peaks on the two mentioned curves must be observed since CO_2 is the only product of the CB combustion both during the fast and slower stages of the reaction. Really, in the absence of other chemical processes (e.g., partial oxidation of carbon), the amount of heat generated because of the $C + O_2 = CO_2$ exothermic reaction is proportional to the amount of CO_2 formed as a result of this reaction. Obviously, the amount of heat generated at each of two stages of the reaction must be comparable with the amount of CO_2 formed at these stages. The integration of the corresponding curves has shown that the first/second peak area ratio was higher for the DTA curves than for the curves of CO_2 formation rate. The observable disproportion between peak areas on the two double-peak curves can be a consequence of overheating the samples at the beginning of their oxidation. Indeed, the first stage of the reaction of CB oxidation is very fast. Apparently, heat production and heat accumulation during this stage are more pronounced than during the second slower oxidation stage, and this can lead to overheating the sample and, hence, to the additional emission of heat.

According to Neeft *et al.* [10], who developed a model describing heat- and mass-transfer between the carbonaceous sample and the surroundings for thermoanalytical techniques, observable double-peak oxidation profiles are a result of combined heat- and mass-transport limitations. The occurrence of both types of limitations can be diminished by using a traditional flow-reactor technique, in which heat transfer is improved since reaction gas flows through the sample and not around it as in DTA experiments [2, 10]. We have carried out TPO experiments under reaction conditions similar to those used in DTA. Indeed, usually, the thermal runaway reaction is not observed in traditional flow-reactor experiments, such as TPO [6, 11, 12].

As expected, in the TPO experiments, we observed only one broad peak on the temperature dependence of the CO_2 formation rate, not two as in the corresponding

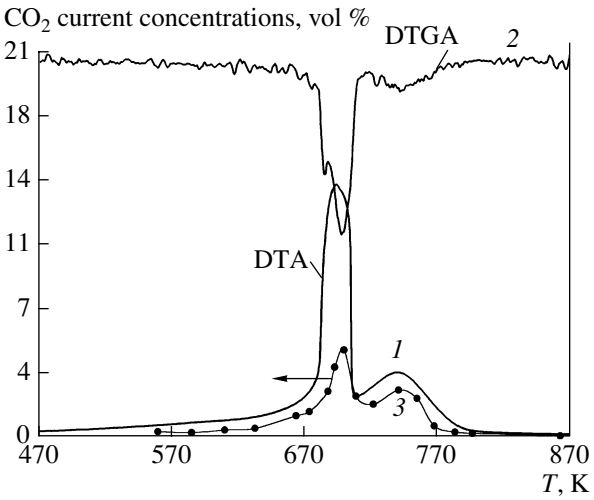

Fig. 1. (*1*) DTA curve and (*2*) DTGA curve for the mixture of CB with the 3%Cu/Y-10 catalyst in air flow and (*3*) CO_2 current concentration measured during the DTA test.

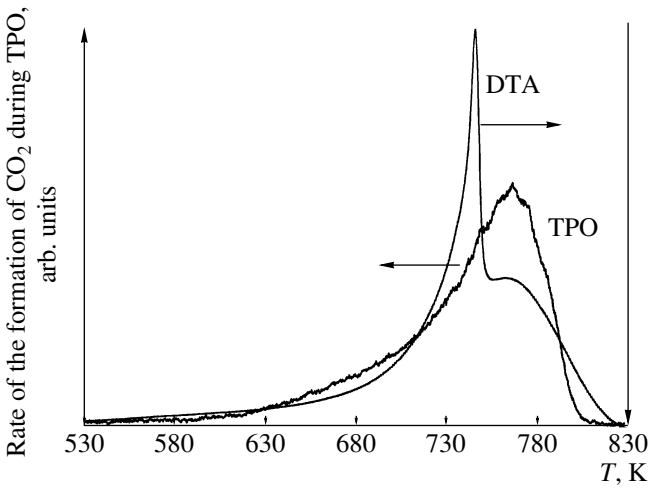

Fig. 2. DTA and TPO curves for the mixture of CB with Y-10 support.

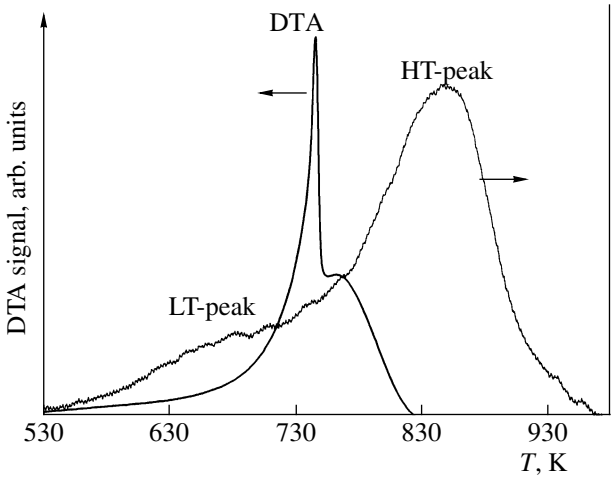

Fig. 3. DTA curve for the mixture of CB with Y-10 support and TPR curve for Y-10.

DTA tests (compare, e.g., the curves of Fig. 2). In Fig. 2, we exploited the DTA curve instead of the curve of the rate of formation of CO_2 during DTA tests since the latter consists of small number of points and, therefore, is less exact. It was found that the maxima temperatures of the TPO peaks were close to the maximum temperatures of the second DTA peaks. Furthermore, the temperatures of the beginning of CO_2 formation were near to those of CB ignition in DTA tests. It is indicated that the presence of two overlapped peaks on the DTA curves is really related to the above-mentioned limitations, leading to a runaway reaction in the low-temperature area.

It has been found that the support itself can act as an oxygen supplier for carbon oxidation. It implies a contribution of a surface redox mechanism (in which the support is reduced by carbon particles with the subsequent reoxidation of the partially reduced surface by gas-phase oxygen) in the overall reaction. Two factors are important for the participation of surface oxygen of the support in the oxidation of carbon. The first one is a good contact between carbon particles and catalyst so that the oxygen of the catalyst could react with the carbon [1–3, 7]. The second essential factor is the presence of a sufficient amount of highly reactive oxygen onto the solid surface to sustain the reaction [13].

The data about oxygen reactivity (determined as reducibility of Ce^{4+} ions) for both pure and metal-loaded Y-10 samples were obtained by TPR technique. TPR curve of Y-10 support consists of two peaks (Fig. 3). The low-temperature (LT) peak characterizes the reducibility of surface Ce^{4+} ions, whereas the high-temperature (HT) one is related to the reduction of Ce^{4+} ions in the support bulk [13, 14]. The maxima of the LT and HT peaks correspond to the temperatures at which the reactivity of the surface and, respectively, bulk oxygen is maximal. As can be seen in Fig. 3, in the temperature range of evolution of the DTA curve, the surface oxygen of the Y-10 support is reactive and, therefore, it can be easily released by the support for the oxidation of carbon.

It also follows from Fig. 3 that, in the temperature range of the occurrence of carbon oxidation, the reactivity of the bulk oxygen of Y-10 is negligible, which is related to low oxygen mobility in its crystal lattice under these conditions and, hence, with the complicated diffusion of oxygen from the support bulk to the surface. The fact that lattice oxygen can be released by the support at rather high temperatures (which are higher than the temperature at the end of the catalytic reaction) excludes its participation in the reaction. A comparison of the maximum temperatures of the second DTA peaks with the temperatures corresponding to the maximal reactivity of oxygen in the bulk of other catalysts (Fig. 4) also indicated a low probability of participation of bulk oxygen of the different catalysts in carbon oxidation (except for 3% V/Y-10 sample). Indeed, for 3% V/Y-10 sample, negligible difference between both temperatures (T_{max} of HT-TPR peak and second DTA peak, Fig. 4) indicates a rather high reactivity of oxygen in the bulk of the catalyst under reaction conditions and its possible participation in carbon oxidation.

In spite of the fact that surface oxygen of the support is rather reactive under the reaction conditions, its participation in the oxidation of carbon by a redox mechanism is not obvious (Table 1). Nevertheless, it can be suggested for metal-loaded catalysts. Really, in most cases, the total weight loss during the reaction was more than 20%. Considering that transition metal oxides are often involved in a redox mechanism during catalytic CB oxidation [4, 15], the phenomenon can be attributed to the carbothermal reduction of metal ions. However, in the case of Cu-containing samples, the found experimental values of surplus weight loss exceed the theoretical ones calculated for the complete

reduction of all present copper(II) by carbon. This testifies to the reduction of centers of support accompanied by the release of oxygen (mainly from catalyst surface), which can further interact with carbon forming CO_2.

The activity of the metal-loaded Y-10 varied in the following sequence: Cu/Y-10 > V/Y-10 > W/Y-10. It is worth noting that the activity of Cu-containing catalysts correlated with the content of supported copper and the most active catalyst (3% Cu/Y-10) exhibited the lowest surface area (Table 1). An increase in the catalytic activity of the Cu-containing samples accompanied by a decrease in their surface area with increasing copper loading are well explained by the formation of CuO particles on the catalyst surface. Apparently, a promising inhibition effect, related to the decrease of surface area (from 55 to 38 m^2/g), is balanced by the high catalytic potential of CuO in CB oxidation. Indeed, in the same reaction, Pruvost *et al.* [4] clarified the role of small CuO particles, whose presence on oxide supports (besides isolated copper species) appeared as a determining parameter versus the activity.

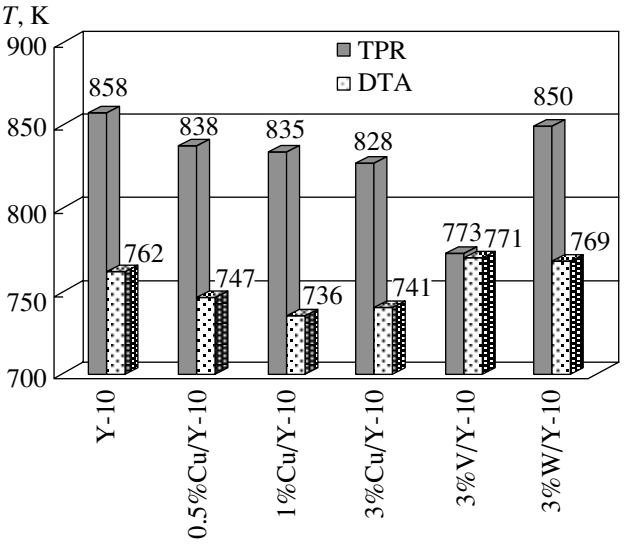

Fig. 4. Temperatures of maxima of second DTA and TPR peaks.

3.2. Analysis of EPR Spectra of Catalysts before and after Catalysis

EPR spectra of initial catalysts (not mixed with carbon black) were recorded after preliminary calcination (at 873 K) in air with subsequent outgassing (~3×10^{-5} mbar). Figure 5 shows the spectra recorded at 77 K.

The spectrum of Y-10 support consists of three signals denoted as *A*, *B*, and *C*. *A* signal at $g = 4.29$ with peak-to-peak width $\Delta H_{pp} = 24.4$ G is attributed to high-spin Fe^{3+} ions ($3d^5$ electronic configuration, $^6S_{5/2}$ ground state, $S = 5/2$) with low-symmetry crystalline field of ligands [16]. *B* signal is an axial anisotropic spectrum with a poorly resolved hyperfine structure. The EPR parameters ($g_\perp = 2.068$, $g_\parallel = 2.277$, $A_\parallel = 150$ G) are characteristic of isolated Cu^{2+} ions ($3d^9$) in distorted octahedral coordination [8]. Fe^{3+} and Cu^{2+} species are present in the support as impurities. *C* signal represents an axial symmetry spectrum with the following parameters: $g_\perp = 1.973$, $g_\parallel = 1.953$. It can be attributed to Zr^{3+} ions ($4d^1$) in an octahedral environment with strong tetragonal distortion [16–20]. The Zr^{3+} ions can be formed during the synthesis of the support, probably due to dehydration of a hydroxide mixture (OH^- groups can play the role of a reducing agent for Zr^{4+} species in hydrated sample [16, 18]).

The spectrum of the 3% W/Y-10 catalyst (not shown) was similar to the Y-10 spectrum, indicating the presence of the above-mentioned ions and the absence of paramagnetic species of tungsten.

As to the 3% Cu/Y-10 catalyst, an intense anisotropic signal is present in the EPR spectrum, and because of its high intensity, the contributions of the *A*, *B*, and *C* signals in the total spectrum are negligible. The parameters of this signal ($g_\perp = 2.1$, $A_\perp \sim 12$ G; $g_\parallel = 2.3$; $A_\parallel \sim 115$ G) were determined by comparison of the experimental spectrum with a simulated one. It was stated that the signal is related to isolated Cu^{2+} ions having a tetragonally distorted octahedral local environment with a rather strong interatomic interaction [8]. Considering the sample preparation conditions, one must suppose that all supported copper is in the Cu^{2+} oxidation state, but not all available copper(II) is visible in the EPR spectrum because of the presence of CuO particles with an antiferromagnetic interaction [8].

A new anisotropic signal with hyperfine structure was observed in an EPR spectrum of the 3% V/Y-10 catalyst in addition to *A*, *B*, and *C* signals. In accordance with the spectral parameters ($g_\perp = 1.983$, $A_\perp = 45$ G; $g_\parallel = 1.933$, $A_\parallel = 170$ G), determined by fitting the spectrum to the simulated one, the signal is typical of paramagnetic V^{4+} ions ($3d^1$) and can be attributed to tetragonally compressed octahedral complexes of vanadyl type VO^{2+} [21]. From the integral intensity of the V^{4+} EPR signal, it was found that a negligible part of the metal was in the V^{4+} oxidation state. The rest of the vanadium was obviously in the V^{5+} oxidation state.

EPR spectra of the catalysts mixed with carbon black after their use in the catalytic oxidation of carbon black (temperature of the end of the reaction was 873 K) were recorded at 77 K after preliminary outgassing (~4×10^{-5} mbar). All the spectra are composed of 4 signals (Fig. 6): The *A*, *B*, and *C* signals described above and attributed to the Fe^{3+}, Cu^{2+}, and Zr^{3+} ions, respectively, and a new broad structureless *X* signal (parameters are given in Table 2).

As follows from the EPR spectra (Fig. 6), admixture Fe^{3+} and Cu^{2+} ions (*A* and *B* signals) are present in all the catalysts (in the case of the 3% Cu/Y-10 sample these signals are not visible because of their low relative intensity). It was found that the intensities of the *A*

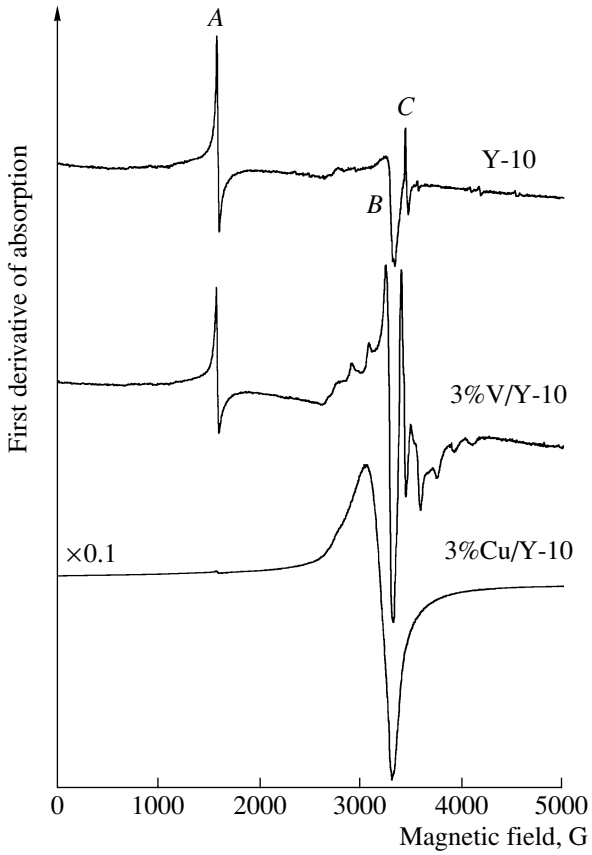

Fig. 5. EPR spectra of initial catalysts (not mixed with carbon black) calcined at 873 K, recorded at 77 K. (Intensities of spectra normalized for sample mass.)

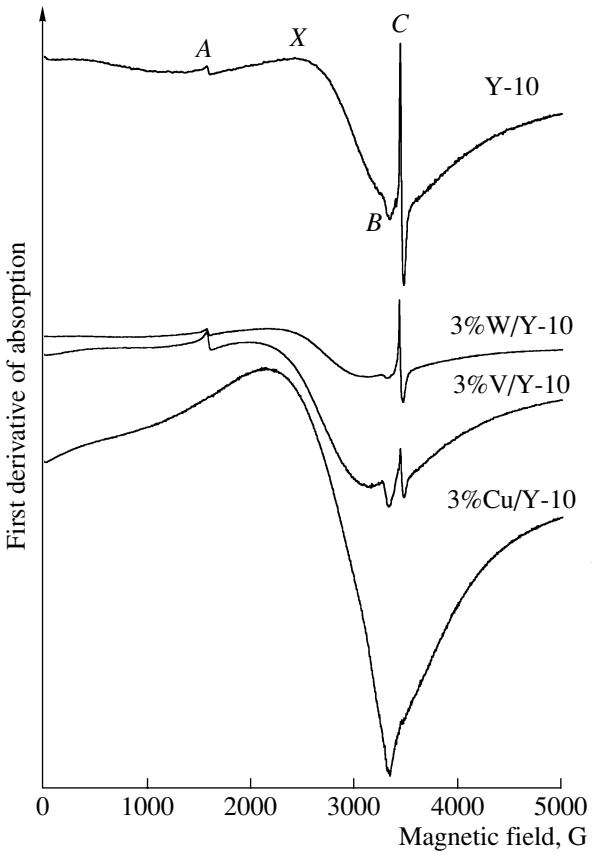

Fig. 6. EPR spectra of the samples (catalyst + CB) after DTA, recorded at 77 K. (Intensities of spectra normalized for sample mass.)

and *B* signals in the EPR spectra of the catalysts used in CB oxidation became significantly lower. This allows one to suppose that the admixture Fe^{3+} and Cu^{2+} ions are reduced by carbon during the reaction.

On the contrary, the amount of Zr^{3+} ions is considerably (~10 times) increased in the Y-10 and 3% W/Y-10 catalysts after CB oxidation compared with that in the initial catalysts (in EPR spectra of the initial Cu- and V-doped samples, the signal from Zr^{3+} is not very visible and, therefore, it is difficult to estimate quantitatively the increase of the amount of Zr^{3+} ions during catalysis). This indicates the pronounced carbothermic reduction of Zr^{4+} ions during the reaction in spite of the strong oxidizing atmosphere. This is in agreement with the literature data [18], where it is reported that surface Zr^{3+} ions of ZrO_2 oxide are quite stable towards molecular oxygen and tend to be coordinatively saturated by various adsorbing species (e.g., CO_2) rather than being oxidized.

Taking into account the trend of the above ions to be carbothermally reduced, one can suppose that the absence of paramagnetic forms of copper and vanadium, in, respectively, the 3% Cu/Y-10 and 3% V/Y-10 used catalysts, is related to the reduction of supported metal species by carbon during the CB oxidation. This in its turn confirms the fact that the reaction is implemented through a redox mechanism with the participation of the supported transition metals. In accordance with the reported data [4, 22], Cu^{2+} ions are the active sites of the 3% Cu/Y-10 catalyst. In the case of the 3% V/Y-10 catalyst, V^{5+} species (and possibly V^{4+}) can play this role [6]. As to the 3% W/Y-10 catalyst, considering the synthesis conditions (see Subsection 2.1), tungsten is expected to be present in the fully oxidized (W^{6+}) state in the initial catalyst; however, we can only suppose that this form of tungsten is weakly active for CB combustion.

Table 2 shows the values of *g*-factors, the peak-to-peak line widths (ΔH_{pp}), and the relative integral intensities of the *X* signal (evaluated as $I(\Delta H_{pp})^2$, where *I* represents the line amplitude) for the tested catalysts. This signal is due to the presence of a paramagnetic form of the residual carbon or/and sulfur compounds. However, the nature of the paramagnetic centers is uncertain. Similar signals have been observed in the EPR spectra of Cu–Ce–Al–O catalysts used in CB oxidation and have been attributed to paramagnetic sulfur compounds [23]. All EPR parameters of *X* signal vary in a wide

Table 2. Spectral parameters of *X* signal

Sample	*g*-Factor	ΔH_{pp}, G	Relative integral intensity normalized for sample mass
CB + Y-10 (after test)	2.2557	1017	6
CB + 3%Cu/Y-10 (after test)	2.3505	1153	72
CB + 3%V/Y-10 (after test)	2.6270	1163	30
CB + 3%W/Y-10 (after test)	2.5028	924	21

range depending on the type of catalyst (Table 2). *X* signal can be related to the presence of paramagnetic metal–carbon or/and metal–sulfur complexes, where the metal is copper, vanadium, tungsten, or impurities. The composition of these complexes and, therefore, the temperature dependence of the corresponding *X* signal in different catalysts are not the same: in the Y-10, 3% Cu/Y-10, and 3% V/Y-10 samples, the intensity of *X* signal increases, while in the 3% W/Y-10 catalyst it decreases with a decrease of recording temperature. It is interesting to note that the quantity of the paramagnetic complexes determined at 293 K increases in the following sequence: Y-10 < W- < V- < Cu-containing catalysts, correlating thus with catalytic activity of the samples.

4. CONCLUSIONS

The temperature of CB combustion was considerably decreased in the presence of all the catalysts. The catalytic activity increased in the following sequence: Y-10 < W- < V- < Cu-containing catalysts, and, for Cu/Y-10 samples, it correlated with the content of the supported metal that was partly related to the CuO formation. The catalytic oxidation of CB occurs in two successive stages related mainly to the oxidation of carbon particles, and the appearance of the fast process during DTA was attributed to a runaway reaction caused by heat- and mass-transfer limitations. For Cu- and V-containing catalysts, a contribution of a surface redox mechanism in the overall reaction was proposed. Cu^{2+} and V^{5+} ions are active sites of Cu- and V-loaded samples, respectively, whereas W^{6+} species are suspected to be responsible for the catalytic activity of the 3% W/Y-10 catalyst. A new EPR signal, found in the catalysts used in CB oxidation, was attributed to the paramagnetic metal–carbon or/and metal–sulfur complexes (metal is Cu, V, W, or impurities), whose quantity increased with an increase in the catalyst activity.

ACKNOWLEDGMENTS

The European Community (European Regional Development Fund) and the region Nord–Pas de Calais are gratefully acknowledged for their financial support in purchasing the apparatus for catalytic tests.

REFERENCES

1. Neeft, J.P.A., Makkee, M., and Moulijn, J.A., *Fuel Process. Technol.*, 1996, vol. 47, p. 1.
2. Neeft, J.P.A., Van Pruissen, O.P., Makkee, M., and Moulijn, J.A., *Stud. Surf. Sci. Catal.*, 1995, vol. 96, p. 549.
3. Moulijn, J.A., Neeft, J.P.A., and Makkee, M., *Appl. Catal. B*, 1996, vol. 8, p. 57.
4. Pruvost, C., Lamonier, J.F., Courcot, D., *et al.*, *Stud. Surf. Sci. Catal.*, 2000, vol. 130, p. 2159.
5. Mul, G., Neeft, J.P.A., Kapteijn, F., *et al.*, *Appl. Catal. B*, 1995, vol. 6, p. 339.
6. Van Setten, B.A.A.L., Van Dijk, R., Jelles, S.J., *et al.*, *Appl. Catal. B*, 1999, vol. 21, p. 51.
7. Stanmore, B.R., Brilhac, J.F., and Gilot, P., *Carbon*, 2001, vol. 39, p. 2247.
8. Kulyova, S.P., Lunina, E.V., Lunin, V.V., *et al.*, *Chem. Mater.*, 2001, vol. 13, p. 1491.
9. Labaki, M., Siffert, S., Lamonier, J.F., *et al.*, *Appl. Catal. B*, 2003 (in press).
10. Neeft, J.P.A., Hoornaert, F., Makkee, M., and Moulijn, J.A., *Therm. Acta*, 1996, vol. 287, p. 261.
11. Li, C. and Brown, T.C., *Carbon*, 2001, vol. 39, p. 725.
12. Badini, C., Saracco, G., Russo, N., and Specchia, V., *Catal. Lett.*, 2000, vol. 69, p. 207.
13. Trovarelli, A., *Catal. Rev. Sci. Eng.*, 1996, vol. 38, p. 439.
14. Vidmar, P., Fornasiero, P., Kašpar, J., *et al.*, *J. Catal.*, 1997, vol. 171, p. 160.
15. Ciambelli, P., Corbo, P., Parrella, P., *et al.*, *Therm. Acta*, 1990, vol. 162, p. 83.
16. Matta, J., Lamonier, J.F., Abi-Aad, E., *et al.*, *Phys. Chem. Chem. Phys.*, 1999, vol. 1, p. 4975.
17. Morterra, C., Giamello, E., Orio, L., and Volante, M., *J. Phys. Chem.,* 1990, vol. 94, p. 3111.
18. Sergent, N., Lamonier, J.F., and Aboukaïs, A., *Chem. Mater.*, 2000, vol. 12, p. 3830.
19. Chen, F.R., Coudurier, G., Joly, J.F., and Vedrine, J.C., *J. Catal.*, 1993, vol. 143, p. 616.
20. Bobricheva, I.V., Stavitsky, I.A., Yermolaev, V.K., *et al.*, *Catal. Lett.*, 1998, vol. 56, p. 23.
21. Bogomolova, L.D., Stefanovsky, S.V., Trool, A.Y., and Vance, E.R., *J. Mater. Sci.*, 2001, vol. 36, p. 1213.
22. Courcot, D., Abi-Aad, E., Capelle, S., and Aboukaïs, A., *Stud. Surf. Sci. Catal.*, 1998, vol. 116, p. 625.
23. Decarne, C., *PhD Dissertation*, Dunkerque: Univ. of Littoral, 2002.